Self-energy of phonons in an anharmonic crystal of order λ^4. II. An application to a monatomic linear chain*

M. R. Monga and K. N. Pathak
Department of Physics, Panjab University, Chandigarh-160014, India
(Received 6 June 1977)

The anharmonic contributions of $O(\lambda^4)$ to the phonon frequency shift and width at high temperatures have been evaluated for a monatomic-linear-chain model. It has been possible to evaluate most of the contributions analytically in an exact and closed form. The remaining contributions have been computed numerically. It is found that the inband phonon width of $O(\lambda^4)$ depends on the wave number contrary to the $O(\lambda^2)$ contribution. The numerical results are used to obtain the magnitudes of all contributions to the inband phonon shift and width at $k = \pi$ for Lennard-Jones systems. A lower-order approximation is found to be inadequate at temperatures about one third of the melting temperature. Our results also show that all anharmonic contributions of $O(\lambda^4)$ are of the same order of magnitude and strongly cancel each other.

I. INTRODUCTION

Recently there has been interests in the study of higher-order anharmonic effects in solids.[1-9,15] In the first paper of this series, one of us[7] has derived general expressions for all anharmonic contributions of $O(\lambda^4)$ to the self-energy of phonons. A detailed analysis of the phonon self-energy is needed to understand various dynamical properties of crystals, for example, the magnitude and temperature dependence of the width of the infrared absorption spectra in ionic crystals; but so far the anharmonic contributions of only a few diagrams of $O(\lambda^4)$ have been examined,[1,2,10] the reason being that the expressions involved are quite lengthy and their numerical evaluation is known to be couplex procedure for realistic models of solids. Therefore the purpose of this paper is to carry out an exact evaluation of all the anharmonic contributions of $O(\lambda^4)$ to the phonon frequency shift and width at high temperature for a nontrivial model of a monatomic linear chain with nearest-neighbor interaction. Our model, although simple, provides guidelines for more realistic three-dimensional calculations. It has been possible to evaluate most of the contributions of $O(\lambda^4)$ analytically and in closed form. A few most complicated contributions are evaluated partly analytically and partly numerically. The contributions to $O(\lambda^4)$ to the phonon frequency shift and width due to thermal expansion also have been obtained.

It is found that the contribution of $O(\lambda^4)$ to the inband phonon width depends on the wave number. The corresponding contribution of $O(\lambda^2)$ is known to be independent of wave number. In order to get an idea of the magnitude of the anharmonic contributions of $O(\lambda^4)$ to the phonon frequency shift and width, we calculate them at $\omega = \omega_k$ and $k = \pi$ for Lennard-Jones systems. It is found that all anharmonic contributions of $O(\lambda^4)$ are of the same order of magnitude and there is strong cancellation among them. Thus none of them can be ignored.

Expressions for anharmonic contributions of $O(\lambda^4)$ to the phonon frequency shift and width at high temperature for monatomic-linear-chain model are given in Sec. II. The calculations, the numerical procedure, and the results are described in Sec. III. Section IV contains discussions and conclusions.

II. EXPRESSIONS FOR THE PHONON SELF-ENERGY AT HIGH TEMPERATURES

The nth order Fourier-transformed anharmonic force constant for a one-dimensional monatomic lattice in the nearest-neighbor approximation can be written as

$$V_n(k_1, k_2, \cdots, k_n) = \frac{N\phi^n(2i)^n}{n!}\left(\frac{\hbar}{2MN}\right)^{n/2}\frac{\sin k_1' \sin k_2' \cdots \sin k_n'}{(\omega_1\omega_2\cdots\omega_n)^{1/2}} \times e^{-i(k_1+k_1+\cdots+k_n)/2}\Delta(k_1+k_2+\cdots+k_n), \quad (1)$$

where $k_1' = \frac{1}{2}k_i$, ϕ^n is the nth-order derivative of the potential energy at the equilibrium position, and

$$\Delta(k) = \begin{cases} 1 & \text{for } k = 0 \text{ or } k \text{ a reciprocal-lattice vector} \\ 0 & \text{otherwise.} \end{cases}$$

The normal-mode frequencies are $\omega_i = \omega_L|\sin k_i'|$ and k_i is restricted to the first Brillouin zone, i.e., $-\pi \le k_i \le \pi$.

A. Frequency-independent self-energy

Substituting V_n from Eq. (1) into Eqs. (31), (32), and (21b) of Ref. 7 (hereafter referred to as I),

the anharmonic contributions of $O(\lambda^4)$ to the phonon self-energy are obtained:

$$P_k^{1b}(\omega) = -(\beta\hbar C_1/16)(\omega_k/\beta^2), \tag{2}$$

$$P_k^{2c}(\omega) = (\beta\hbar C_2/8)(\omega_k/\beta^2), \tag{3}$$

$$P_k^{2e}(\omega) = \beta\hbar C_3/12)(\omega_k/\beta^2), \tag{4}$$

where $C_1 = \phi''''/(\phi'')^3$, $C_2 = (\phi''')^2/(\phi'')^4$, $C_3 = \phi'''\phi''''/(\phi'')^4$, and $\omega_k = \omega_L|\sin(\frac{1}{2}k)|$. Here and in what follows we use the notations of I. Equation (2) correspond to diagram (1b) whereas Eqs. (3) and (4) are the results of the diagrams (2c) and (2e) of I. The last frequency-independent contribution to the phonon self-energy corresponding to diagram (3d) is given by Eq. (27a) of I. After taking due care of the repeated pole, the expression for this contribution is found to be

$$P_{kk'}^{3d}(\omega) = -\frac{216\beta\lambda^4}{\hbar^2}\sum_{q_1,q_2,q_3} V_4(-k,q_2,-q_2,k')V_3(-q_1,q_2,-q_3)V_3(q_1,-q_2,q_3) \times \sum_{p_1p_2p_3} p_1p_3\left(\frac{(1+n_{p_1})(1+n_{p_3})+n_{p_2}(1+n_{p_1}+n_{p_3})}{(p_1\omega_1+p_2\omega_2+p_3\omega_3)^2} + \frac{\beta\hbar n_{p_2}(1+n_{p_2})(1+n_{p_1}+n_{p_3})}{p_1\omega_1+p_2\omega_2+p_3\omega_3} + \frac{n_{p_2}(1+n_{p_1}+n_{p_3})+(1+n_{p_1})(1+n_{p_3})}{p_2\omega_2(p_1\omega_1+p_2\omega_2+p_3\omega_3)}\right). \tag{5}$$

In the high-temperature limit Eq. (5) reduces to

$$P_{kk'}^{3d}(\omega) = -\frac{216\times 16\beta}{\beta^2\hbar^4}\sum_{q_1,q_2,q_3} V_4(-k,q_2,-q_2,k')V_3(-q_1,q_2,-q_3)V_3(q_1,-q_2,q_3)(\omega_1\omega_2^2\omega_3)^{-1}. \tag{6}$$

For the model of a monatomic linear chain, Eq. (6) is found to be

$$P_k^{3d}(\omega) = -\frac{\beta\hbar C_4}{8}\frac{\omega_k}{\beta^2}, \tag{7}$$

where $C_4 = \phi''''(\phi''')^2/(\phi'')^5$.

B. Frequency-dependent self-energy

The frequency-dependent self-energy corresponding to diagram (2b) is obtained from Eq. (19b) of I and it is written as

$$P_k^{2b}(\omega) = -\frac{\beta\hbar C_2}{96}\frac{\omega_k}{\beta^2}\frac{1}{4\pi^2} \times \int_{-\pi}^{\pi}\int_{-\pi}^{\pi} dq_1\,dq_2 \sum_{p_1p_2p_3}\frac{p_1\omega_1+p_2\omega_2+p_3\omega_{k-1-2}}{\omega+p_1\omega_1+p_2\omega_2+p_3\omega_{k-1-2}}, \tag{8}$$

where $\omega_{k-1-2} = |\sin\frac{1}{2}(k-q_1-q_2)|$ and ω is defined in units of the maximum frequency ω_L. This is a second-order quartic anharmonic contribution. In second-order perturbation there is another contribution which corresponds to a cubic fifth-order term in the Hamiltonian and is represented by diagram (2d) of I. From Eq. (34) of I we obtain it as

$$P_k^{2d}(\omega) = -\frac{\beta\hbar C_3}{32}\frac{\omega_k}{\beta^2}\frac{1}{\pi}\int_{-\pi}^{\pi} dq_1 \sum_{p_1p_2}\frac{p_2\omega_{k-1}-p_1\omega_1}{\omega+p_1\omega_1-p_2\omega_{k-1}}, \tag{9}$$

where $\omega_{k-1} = |\sin\frac{1}{2}(k-q_1)|$.

In third-order perturbation theory there are three diagrams (3a), (3b), and (3c). The contribution corresponding to diagram (3a) is given by the expression (35) of I, which for our model can be written as

$$P_k^{3a}(\omega) = -\frac{\beta\hbar C_4}{128}\frac{\omega_k}{\beta^2} \times \left(\frac{1}{2\pi}\int_{-\pi}^{\pi} dq_1 \sum_{p_1p_2}\frac{p_2\omega_{k-1}-p_1\omega_1}{\omega+p_1\omega_1-p_2\omega_{k-1}}\right)^2. \tag{10}$$

The contribution of diagrams (3b), after taking due care of the repeated pole, is obtained as

$$P_{kk'}^{3b}(\omega) = -\frac{216\beta}{\hbar^2}\sum_{q_1,q_3,q_4} V_3(-k,q_1,q_4)V_4(-q_1,q_3,-q_3,q_1)V_3(-q_1,-q_4,k') \times \sum_{p_1p_3p_4} p_3p_4n_{p_3}\left(\frac{1+n_{p_1}+n_{p_4}}{(\omega+p_1\omega_1+p_4\omega_4)^2} + \frac{\beta\hbar n_{p_1}(1+n_{p_1})}{\omega+p_1\omega_1+p_4\omega_4} + \frac{1+n_{p_1}+n_{p_4}}{p_1\omega_1(\omega+p_1\omega_1+p_4\omega_4)}\right). \tag{11}$$

Equation (11) for a monatomic-linear-lattice model is found to be

$$P_k^{3b}(\omega) = -\frac{\beta\hbar C_4}{64}\frac{\omega_k}{\beta^2}\left[\frac{1}{2\pi}\int_{-\pi}^{\pi}\sum_{p_1 p_2}\left(\frac{2(p_1\omega_1+p_2\omega_{k-1})}{\omega+p_1\omega_1+p_2\omega_{k-1}} - \frac{\omega p_1\omega_1}{(\omega+p_1\omega_1+p_2\omega_{k-1})^2}\right)\right]. \tag{12}$$

The last third-order contribution corresponding to diagram (3c) is obtained from Eq. (37) of I which for our model is

$$P_k^{3c}(\omega) = -\frac{\beta\hbar C_4}{32}\frac{\omega_k}{\beta^2}\frac{1}{4\pi^2} \times \int_{-\pi}^{\pi}\int_{-\pi}^{\pi} dq_1\, dq_2\left[\sum_{p_1 p_2 p_3 p_4}\left(\frac{p_1\omega_1+p_2\omega_{2-1}}{p_1\omega_1+p_2\omega_{2-1}-p_4\omega_2}\,\frac{p_3\omega_{k-2}+p_4\omega_2}{\omega+p_3\omega_{k-2}+p_4\omega_2} - \frac{p_4\omega_2(p_1\omega_1+p_2\omega_{2-1}+p_3\omega_{k-2})}{(\omega+p_1\omega_1+p_2\omega_{2-1}+p_3\omega_{k-2})(p_1\omega_1+p_2\omega_{2-1}-p_4\omega_2)}\right)\right] \tag{13}$$

In fourth-order perturbation there are two diagrams (4a) and (4b) which arise from the cubic anharmonic term in the Hamiltonian. The contribution corresponding to diagram (4a) is given by Eq. (28b) only for $p_1\omega_1 \neq p_5\omega_5$. For the case $p_1\omega_1 = p_5\omega_5$, taking due care of the repeated pole of order 2, we obtain the expression

$$\begin{aligned} P_{kk'}^{4a}(\omega) = \frac{648\beta}{\hbar^3}\sum_{q_1 q_2 q_3 q_4} & V_3(-k,q_1,q_2)V_3(-q_1,q_3,q_4)V_3(-q_3,q_4,q_1)V_3(-q_1,-q_2,k') \\ & \times \sum_{p_1 p_2 p_3 p_4} p_2 p_3 p_4 \left\{\frac{1}{\omega+p_2\omega_2+p_3\omega_3+p_4\omega_4}\left[\frac{n_{p_2}(1+n_{p_3}+n_{p_4})}{(\omega+p_1\omega_1+p_2\omega_2)^2} + \frac{n_{p_2}(1+n_{p_3}+n_{p_4})}{p_1\omega_1(\omega+p_1\omega_1+p_2\omega_2)}\right.\right. \\ & \left. + (1+n_{p_3})(1+n_{p_4})\left(\frac{1}{(p_4\omega_4+p_3\omega_3+p_1\omega_1)^2} + \frac{1}{p_4\omega_4+p_3\omega_3+p_1\omega_1}\right)\right] \\ & + \frac{(1+n_{p_1})(1+n_{p_3}+n_{p_4})}{(\omega+p_1\omega_1+p_2\omega_2)(p_4\omega_4+p_3\omega_3+p_1\omega_1)} \\ & \left.\times\left(\frac{1}{\omega+p_1\omega_1+p_2\omega_2} + \frac{1}{p_4\omega_4+p_3\omega_3+p_1\omega_1} + \frac{1}{p_1\omega_1} + \beta\hbar n_{p_1}\right)\right\}. \end{aligned} \tag{14}$$

For a monatomic linear chain and at high temperature, the above equation reduces to

$$P_k^{4a}(\omega) = \frac{\beta\hbar C_5}{128}\frac{\omega_k}{\beta^2}\frac{1}{4\pi^2}\left[\int_{-\pi}^{\pi}\int_{-\pi}^{\pi} dq_1\, dq_2 \sum_{p_1 p_2 p_3 p_4}\left(2 - 2\omega A_{p_1 p_2} - \omega p_1\omega_1 A_{p_1 p_2}^2 - \frac{\omega(p_1\omega_1 A_{p_1 p_2} + \omega_1^2 A_{p_1 p_2}^2)}{\omega+p_2\omega_{k-1}+p_3\omega_{2-1}+p_4\omega_2}\right)\right], \tag{15}$$

where $A_{p_1 p_2} = (\omega+p_1\omega_1+p_2\omega_{k-1})^{-1}$ and $C_5 = (\phi''')^4/(\phi'')^6$. The second and the last anharmonic contribution in fourth-order perturbation corresponding to diagram (4b) is given by Eq. (39) of I. For the present model this is found to be

$$P_k^{4b}(\omega) = \frac{\beta\hbar C_5}{64}\frac{\omega_k}{\beta^2}\frac{1}{4\pi^2} \times \int_{-\pi}^{\pi}\int_{-\pi}^{\pi} dq_1\, dq_2 \sum_{p_1 p_2 p_3 p_4 p_5}\left(\frac{p_4\omega_{k-2}(p_1\omega_1+p_2\omega_{k-1})}{(\omega+p_1\omega_1+p_2\omega_{k-1})(\omega+p_4\omega_{k-2}+p_5\omega_2)} - \frac{\omega p_1\omega_1 p_4\omega_{k-2}}{(\omega+p_1\omega_1+p_2\omega_{k-1})(\omega+p_4\omega_{k-2}+p_5\omega_2)(\omega+p_2\omega_{k-1}+p_3\omega_{1-2}+p_5\omega_2)}\right). \tag{16}$$

The expressions discussed in this section contribute to both phonon frequency shift and width. It may be noted that expressions (5), (11), and (14) which apply to the cases of repeated poles have not been obtained in I. This is why they are given in this section for a general case and for all temperatures which then completes the expressions for all anharmonic contributions of $O(\lambda^4)$ to the phonon self-energy given in I.[11]

are defined as

$$\lim_{\epsilon\to 0^+} -(\beta\hbar)^{-1}P_{kk'}(\omega+i\epsilon)=\Delta_{kk'}(\omega)-i\Gamma_{kk'}(\omega)\,. \quad (17)$$

Using the identity

$$\lim_{\epsilon\to 0^+}(x\pm i\epsilon)^{-1}=P/x\mp i\pi\delta(x)\,, \quad (18)$$

one easily obtains from Eqs. (8)–(10), (12), (13), (15), and (16) the expressions for the real and the imaginary parts of the phonon self-energy. The expression for $\Delta_k(\omega)$ is $-(\beta\hbar)^{-1}P_k(\omega)$ but now it involves the principal values of the integrals. We first calculate the phonon frequency shift $\Delta_k(\omega)$, and the imaginary part $\Gamma_k(\omega)$ is obtained as the Hilbert transform of the real part, i.e.,

$$\Gamma_k(\omega)=-\frac{P}{\pi}\int_{-\infty}^{\infty}d\omega'\,\frac{\Delta_k(\omega')}{(\omega'-\omega)}\,. \quad (19)$$

A. Phonon frequency shift

The frequency-independent contributions to the phonon frequency shift can be read easily from Eqs. (2)–(4) and (7).

We now obtain the closed-form expressions for the frequency-dependent contributions by evaluating the principal values of the integrals appearing in Eqs. (9), (10), and (12). These contributions to the phonon frequency shift have been found to be

$$\Delta_k^{2d}(\omega)=\tfrac{1}{8}C_3(\omega_k/\beta^2)\{\omega[X^{-1/2}\Theta(X)+Y^{-1/2}\Theta(Y)]-2\}\,, \quad (20)$$

where $X=\omega^2-4\cos^2\tfrac{1}{4}k$, $Y=\omega^2-4\sin^2\tfrac{1}{4}k$, and $\Theta(x)$ is defined as

$$\Theta(x)=\begin{cases}1 & \text{for } x>0\\ 0 & \text{for } x\le 0\,,\end{cases} \quad (21)$$

$$\Delta_k^{3a}(\omega)=\tfrac{1}{32}C_4(\omega_k/\beta^2)\{[\omega X^{-1/2}\Theta(X)+\omega Y^{-1/2}\Theta(Y)-2]^2-[\omega X_1^{-1/2}\Theta(X_1)+\omega Y_1^{-1/2}\Theta(Y_1)]^2\}\,, \quad (22)$$

$$\Delta_k^{3b}(\omega)=\tfrac{1}{64}C_4(\omega_k/\beta^2)\{8-5\omega[X^{-1/2}\Theta(X)+Y^{-1/2}\Theta(Y)]+\omega^3[X^{-3/2}\Theta(X)+Y^{-3/2}\Theta(Y)]\}\,, \quad (23)$$

where $X_1=-X$ and $Y_1=Y$. It is convenient to discuss the above anharmonic contributions to the phonon frequency shift with the help of Fig. 1. It is easily seen that in region I neither of the Θ functions is satisfied. This implies that inband modes are only shifted by a constant amount due to anharmonicity. There is a frequency-dependent shift for the modes lying in regions II and III. Further, we note that for $\omega\gg 2$, the anharmonic contributions to the phonon frequency shift given by Eqs. (20) and (23) varies as $1/\omega^2$ whereas Eq. (22) varies as $1/\omega^4$.

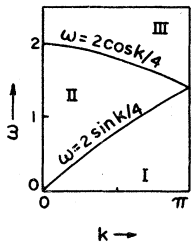

FIG. 1. Regions of validity of the theta functions $\Theta(X)$ and $\Theta(Y)$.

The remaining four frequency-dependent contributions to the phonon frequency shift given by expressions (8), (13), (15), and (16) could not be completely evaluated analytically. For these, it has been possible to carry out one integration. We thus obtain for the second-order quartic anharmonic contribution to the phonon frequency shift

$$\Delta_k^{2b}(\omega)=\tfrac{1}{12}C_2(\omega_k/\beta^2)[4\pi)^{-1}I_R^{2b}(k,\omega)-1]\,, \quad (24)$$

where

$$I_R^{2b}(k,\omega)=\omega\int_0^{\pi}dx\sum_{p_1p_2}[Z_{p_1p_2}(x,k,\omega)]^{-1/2}\times\Theta(Z_{p_1p_2}(x,k,\omega))\,, \quad (25)$$

$$Z_{p_1p_2}(x,k,\omega)=(\omega+p_1\sin x)^2-2[1+p_2\cos(k'-x)]\,, \quad (26)$$

and $k'=\tfrac{1}{2}k$. In the numerical evaluation of the integral appearing in Eq. (25), it is extremely useful to know in advance the ranges in which various Θ functions are satisfied. They are shown in Fig. 2. All the Θ functions are always satisfied in region III and are never satisfied in region I, but they are satisfied in region II in some partial range of x. It is furthermore interesting the note that for $\omega\gg 3$, $\Delta_k^{2b}(\omega)$ behaves as ω^{-2}. The integral $I_R^{2b}(k,\omega)$ has been evaluated numerically for $k=\pi$ using the Gauss quadrature method on the IBM-360 computer. The range of the integration is divided into many proper subranges and the integration is

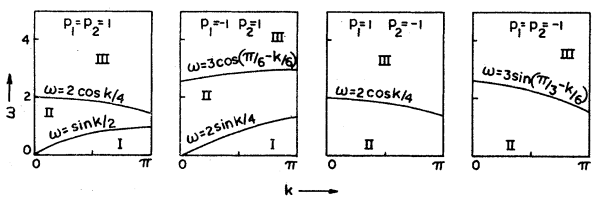

FIG. 2. Regions of validity of the theta functions $\Theta(Z_{p_1p_2}(x,k,\omega))$.

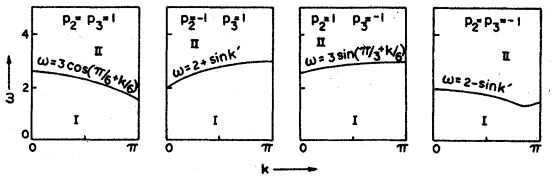

FIG. 3. Regions of validity of the theta functions $\Theta(F_{p_2p_3}(x,k,\omega))$.

made for each subrange. Polynomials of degree 8, 9, 10, 32, and 40 are used in order that the integrated values remain consistent within 5%. A similar numerical procedure has been used for subsequent integrals. The numerical results of $I_R^{2b}(k,\omega)$ for $k=\pi$ are presented in Fig. 4.

The anharmonic contribution to the phonon frequency shift corresponding to Eq. (13), after carrying out one integration, is found to be

$$\Delta_k^{3c}(\omega)=\tfrac{1}{8}C_4(\omega_k/\beta^2)\{4-2\omega[X^{-1/2}\Theta(X)+Y^{-1/2}\Theta(Y)] -I_R^{3c}(k,\omega)\}, \quad (27)$$

where

$$I_R^{3c}(k,\omega)=\frac{\omega}{2\pi}P\int_0^\pi dx \sum_{p_1p_2p_3} B_{p_1p_2}(x,k,\omega) \times[F_{p_2p_3}(x,k,\omega)]^{-1/2} \times\Theta(F_{p_2p_3}(x,k,\omega)). \quad (28)$$

Here

$$F_{p_2p_3}(x,k,\omega)=[\omega+p_2\sin(k'-x)]^2-2(1+p_3\cos x), \quad (29)$$

$$B_{p_1p_2}(x,k,\omega)=(p_1\sin x)/[\omega+p_1\sin x+p_2\sin(k'-x)]. \quad (30)$$

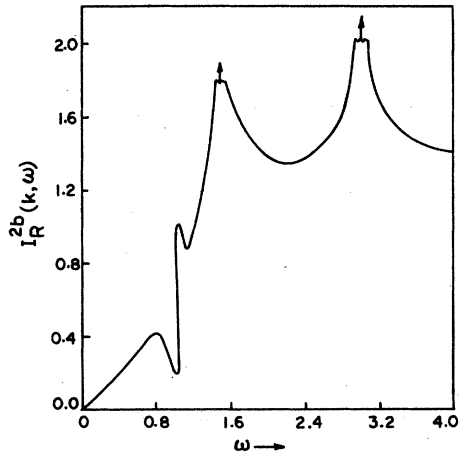

FIG. 4. Plot of $I_R^{2b}(k,\omega)$ vs ω at $k=\pi$. Actual values are 10 times the plotted values.

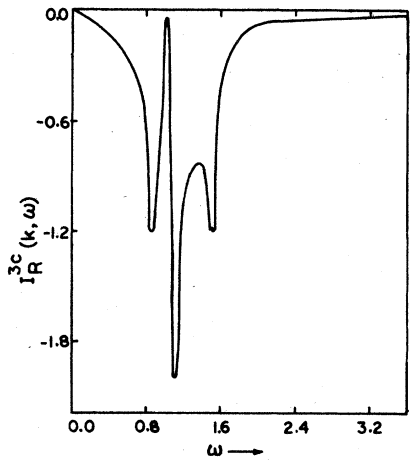

FIG. 5. Variation of $I_R^{3c}(k,\omega)$ at $k=\pi$. Actual values are 10 times the plotted values.

The regions of validity of $\theta(X)$ and $\theta(Y)$ have already been discussed in Fig. 1. The regions of validity of the theta functions appearing in the integrand of Eq. (28) are plotted in Fig. 3.for the whole range of $0\leq x\leq\pi$. These theta functions are always satisfied in region II, but in region I they are satisfied within some partial range of x. The dip in Fig. 3 is due to the competition between the values $3\sin\frac{1}{6}k$ and $2-\sin k'$. These curves intersect at $k=83\pi/120$. Equation (28) has been computed numerically for $k=\pi$ and results are presented in Fig. 5. It may be noted that for $\omega\gg3$, $\Delta_k^{3c}(\omega)$ varies as ω^{-2}.

The next anharmonic contribution to the phonon frequency shift corresponding to Eq. (15) after some lengthy calculation is found as

$$\Delta_k^{4a}(\omega)=-\tfrac{1}{128}C_5(\omega_k/\beta^2)\{32-20\omega[X^{-1/2}\Theta(X)+Y^{-1/2}\Theta(Y)] +4\omega^3[X^{-3/2}\Theta(X)+Y^{-3/2}\Theta(Y)]-I_R^{4a}(k,\omega)\}, \quad (31)$$

where

$$I_R^{4a}(k,\omega)=\frac{2\omega}{\pi}P\int_0^\pi dx \sum_{p_1p_2p_3}[B_{p_1p_2}(x,k,\omega)+B_{p_1p_2}^2(x,k,\omega)] \times[F_{p_2p_3}(x,k,\omega)]^{-1/2} \times\Theta(F_{p_2p_3}(x,k,\omega)). \quad (32)$$

Equation (32) has been computed numerically for $k=\pi$ and $I_R^{4a}(k,\omega)$ vs ω is plotted in Fig. 6. It is seen that for $\omega\gg3$, $\Delta_k^{4a}(\omega)$ varies as ω^{-2}. The last frequency-dependent anharmonic contribution to the phonon frequency shift is obtained from Eq. (16), and after some lengthy and tedious calculation we obtain it is

$$\Delta_k^{4b}(\omega)=-\tfrac{1}{64}C_5(\omega_k/\beta^2)\{[2-\omega X^{-1/2}\Theta(X)-\omega Y^{-1/2}\Theta(Y)]^2 -I_R^{4b}(k,\omega)\}, \quad (33)$$

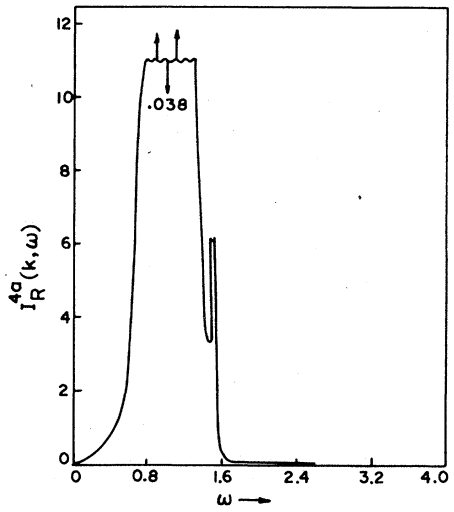

FIG. 6. Variation of $I_R^{4a}(k,\omega)$ with ω at $k=\pi$. Actual values are 100 times the plotted values.

where

$$I_R^{4b}(k,\omega)=\frac{\omega}{2\pi}P\int_0^\pi dx\sum_{p_1p_2}B_{p_1p_2}(x,k,\omega)H(x,k,\omega)\,. \tag{34}$$

$H(x,k,\omega)$, being a lengthy expression, is given in the Appendix. The computed values of $I_R^{4b}(k,\omega)$ for $k=\pi$ are plotted in Fig. 7. It is found that for $\omega\gg 3$, $\Delta_k^{4b}(\omega)$ varies as ω^{-2}.

B. Phonon frequency widths

We have evaluated all the anharmonic contributions to the phonon frequency width using Eq. (19)

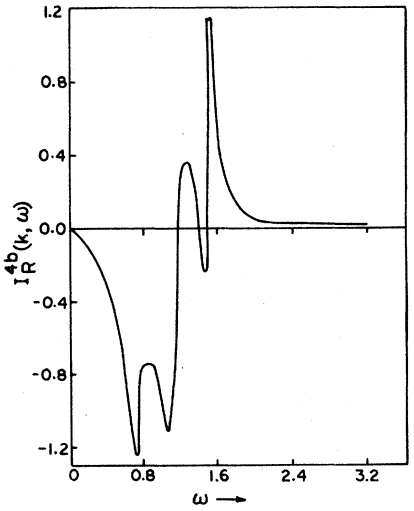

FIG. 7. Plot of $I_R^{4b}(k,\omega)$ vs ω at $k=\pi$. Actual values are 10 times the plotted values.

and the results for the phonon frequency shift given in Sec. III A. The Hilbert transform of the frequency-independent anharmonic contributions to the phonon frequency shift is zero, and thus Eqs. (2)–(4) and (7) do not contribute to the phonon frequency width. The anharmonic contributions to the phonon frequency width corresponding to Eqs. (20), (22), and (23) are found to be

$$\Gamma_k^{2d}(\omega)=\tfrac{1}{8}C_3(\omega_k/\beta^2)[\omega X_1^{-1/2}\Theta(X_1)+\omega Y_1^{-1/2}\Theta(Y_1)]\,, \tag{35}$$

$$\Gamma_k^{3a}(\omega)=\tfrac{1}{16}C_4(\omega_k/\beta^2)\{[\omega X^{-1/2}\Theta(X)+\omega Y^{-1/2}\Theta(Y)-2]\times[\omega X_1^{-1/2}\Theta(X_1)+\omega Y_1^{-1/2}\Theta(Y_1)]\}\,, \tag{36}$$

$$\Gamma_k^{3b}(\omega)=-\tfrac{1}{64}C_4(\omega_k/\beta^2)\{5\omega[X_1^{-1/2}\Theta(X_1)+Y_1^{-1/2}\Theta(Y_1)]+\omega^3[X_1^{-3/2}\Theta(X_1)+Y_1^{-3/2}\Theta(Y_1)]\}\,. \tag{37}$$

The regions in which the theta functions occurring in Eqs. (35)–(37) hold can be discussed with the help of Fig. 1. It can be easily seen that neither of the theta functions $\Theta(X_1)$ and $\Theta(Y_1)$ are satisfied in region III whereas $\Theta(Y_1)$ is satisfied only in region I. But the theta function $\Theta(X_1)$ is satisfied always in region II as well as in region I. It is worth pointing out here that the phonon width at $\omega=\omega_k$ is independent of k for Eqs. (35) and (36), whereas it depends on k for Eq. (37). It may be noted that the inband phonon width is independent of k in lower order.

The remaining four anharmonic contributions to the phonon frequency width could not be completely worked out analytically. However, we get for them expressions involving one integration by taking the Hilbert transform of Eqs. (24), (27), (31), and (33). We obtain the second-order quartic anharmonic contribution to the phonon frequency width as

$$\Gamma_k^{2b}(\omega)=(C_2/48\pi)(\omega_k/\beta^2)I_G^{2b}(k,\omega)\,, \tag{38}$$

where

$$I_G^{2b}(k,\omega)=\omega P\int_0^\pi dx\sum_{p_1p_2}Z'_{p_1p_2}(x,k,\omega)\Theta(Z'_{p_1p_2}(x,k,\omega))\,, \tag{39}$$

$$Z'_{p_1p_2}(x,k,\omega)=-Z_{p_1p_2}(x,k,\omega)\,. \tag{40}$$

The regions in which the theta functions $\Theta(Z'_{p_1p_2}(x,k,\omega))$ are satisfied can be discussed from Fig. 2. None of the theta functions is satisfied in region III whereas all are satisfied in regions I and II either in the whole range or in some partial range of x. Using the procedure discussed earlier, Eq. (39) has been computed numerically and results for $k=\pi$ are plotted in Fig. 8.

The next anharmonic contribution to the phonon frequency width worked out from Eq. (27) can be

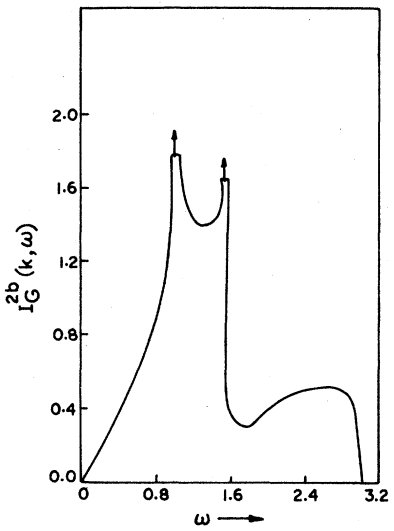

FIG. 8. Variation of $I_G^{2b}(k,\omega)$ with ω at $k=\pi$. Actual values are 10 times the plotted values.

written as

$$\Gamma_k^{3c}(\omega) = -\tfrac{1}{8}C_4(\omega_k/\beta^2)\{2\omega[X_1^{-1/2}\Theta(X_1)+Y_1^{-1/2}\Theta(Y_1)] + I_G^{3c}(k,\omega)\}, \quad (41)$$

where

$$I_G^{3c}(k,\omega) = \frac{\omega}{2\pi}P\int_0^{\pi} dx \sum_{p_1p_2p_3} B_{p_1p_2}(x,k,\omega) \times [F'_{p_2p_3}(x,k,\omega)]^{-1/2} \times \Theta(F'_{p_2p_3}(x,k,\omega)), \quad (42)$$

$$F'_{p_2p_3}(x,k,\omega) = -F_{p_2p_3}(x,k,\omega). \quad (43)$$

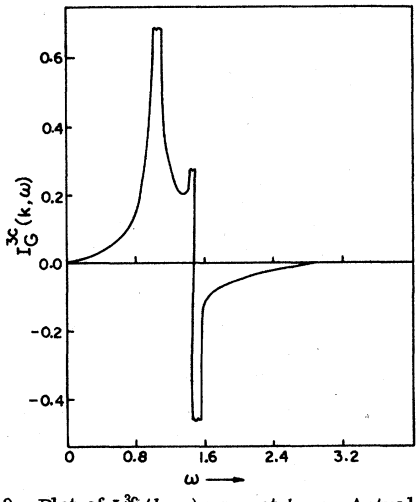

FIG. 9. Plot of $I_G^{3c}(k,\omega)$ vs ω at $k=\pi$. Actual values are 10 times the plotted values.

We note that the region in which the theta functions appearing in Eq. (42) are satisfied in the whole or in some partial range of x is region I of Fig. 3. They are never satisfied in region II. For principal value we use the representation $P/y = y/(y^2+\epsilon^2)$. It is found that values of ϵ lying between 0.001 and 0.02 give computed results for $I_G^{3c}(k,\omega)$ which are consistent within 5%. These are plotted for $k=\pi$ in Fig. 9.

Another anharmonic contribution to the phonon frequency width after taking the Hilbert transform of Eq. (31) is found to be

$$\Gamma_k^{4a}(\omega) = \tfrac{1}{128}C_5(\omega_k/\beta^2)\{20\omega[X_1^{-1/2}\Theta(X_1)+Y_1^{-1/2}\Theta(Y_1)] + 4\omega^3[X_1^{-3/2}\Theta(X_1)+Y_1^{-3/2}\Theta(Y_1)] + 4I_G^{3c}(k,\omega)+I_G^{4a}(k,\omega)\}, \quad (44)$$

where

$$I_G^{4a}(k,\omega) = \frac{2\omega}{\pi}P\int_0^{\pi} dx \sum_{p_1p_2p_3} B^2_{p_1p_2}(x,k,\omega) \times [F'_{p_2p_3}(x,k,\omega)]^{-1/2} \times \Theta(F'_{p_2p_3}(x,k,\omega)). \quad (45)$$

In order to compute Eq. (45) numerically we use the representation

$$P/y^2 = (y^2-\epsilon^2)/(y^2+\epsilon^2)^2, \quad (46)$$

where ϵ is assumed small but finite. With this representation we find that the results for $I_G^{4a}(k,\omega)$ increase monotonically with decreasing ϵ and when ϵ is chosen very small the results behave in an unpredictable way. The reason for this is that though ϵ is assumed small it cannot be smaller than the smallest increment in y. The optimum value of ϵ is dependent on the smallest increment in y. Using Eq. (46) we first compute the principal value of the known integral,

$$J(k,\omega) = P\int_0^{\pi} dx \sum_{p_1p_2} \frac{1}{[\omega+p_1\sin x+p_2\sin(k'-x)]^2}, \quad (47)$$

for $k=\pi$ to determine ϵ. The values of ϵ lying between 0.02 and 0.001 reproduce the known results for the above integral with a 5% consistency for various values of ω. Using these values of ϵ, $I_G^{4a}(k,\omega)$ is computed for $k=\pi$ and the results are presented in Fig. 10. The last anharmonic contribution to the phonon frequency width has been obtained from Eq. (33) using Eq. (19). After lengthy calculations it can be written as

$$\Gamma_k^{4b}(\omega) = -\tfrac{1}{64}C_5(\omega_k/\beta^2)\{2\omega^2(X_1Y)^{-1/2}\Theta(X_1)\Theta(Y) - 4\omega[X_1^{-1/2}\Theta(X_1)+Y_1^{-1/2}\Theta(Y_1)] - I_G^{4b}(k,\omega)\}, \quad (48)$$

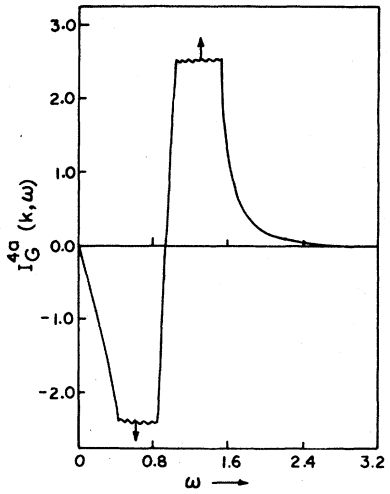

FIG. 10. Plot of $I_G^{4a}(k,\omega)$ vs ω at $k=\pi$. Actual values are 10 times the plotted values.

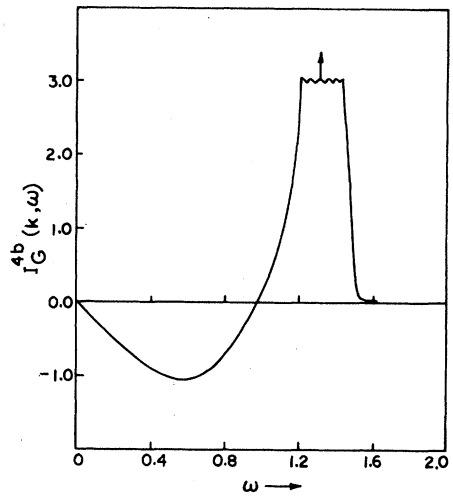

FIG. 11. Variation of $I_G^{4b}(k,\omega)$ with ω at $k=\pi$. Actual values are 100 times the plotted values.

where

$$I_G^{4b}(k,\omega)=\frac{\omega}{2\pi}P\int_0^{\pi}dx\sum_{p_1p_2}B_{p_1p_2}(x,k,\omega)H_1(x,k,\omega)\,. \tag{49}$$

$H_1(x,k,\omega)$ can be read from Eq. (A25) in the Appendix. The computed values of $I_G^{4b}(k,\omega)$ consistent within 5% for $k=\pi$ are presented in Fig. 11.

The derivatives of the potential ϕ^n occurring in the expression for phonon frequency shift and width given in this section are evaluated at the nearest-neighbor separation r_0 at temperature T. Therefore it is necessary to expand the derivatives about the minimum of the potential energy at $\bar{r}_0$. Thus we obtain the so-called thermal-expansion contribution to $O(\lambda^4)$ to the phonon frequency shift Δ^{TE} and width Γ^{TE} as

$$\Delta_2^{TE}=0.5\omega_k aT\bar{r}_0\phi'''(\bar{r}_0)/\phi''(\bar{r}_0)\,, \tag{50}$$

$$\begin{aligned}\Delta_4^{TE}=&\,0.25\frac{\omega_k}{\beta}\left[aT\bar{r}_0\left(\frac{\phi''''(\bar{r}_0)}{[\phi''(\bar{r}_0)]^2}-3.5\frac{\phi'''(\bar{r}_0)\phi'''(\bar{r}_0)}{[\phi''(\bar{r}_0)]^3}+2.5\frac{[\phi'''(\bar{r}_0)]^3}{[\phi''(\bar{r}_0)]^4}\right)\right]\\&+0.5\omega_k\left\{\frac{bT^2r_0\phi'''(\bar{r}_0)}{\phi''(\bar{r}_0)}+0.25a^2T^2\bar{r}_0^2\left[\frac{2\phi''''(\bar{r}_0)}{\phi''(\bar{r}_0)}-\left(\frac{\phi'''(\bar{r}_0)}{\phi''(\bar{r}_0)}\right)^2\right]\right\}\\&+0.125\frac{\omega_k}{\beta}\omega aT\bar{r}_0\left[[X^{-1/2}\Theta(X)+Y^{-1/2}\Theta(Y)]\left(\frac{2\phi'''(\bar{r}_0)\phi''''(\bar{r}_0)}{[\phi''(\bar{r}_0)]^3}-2.5\frac{[\phi'''(\bar{r}_0)]^3}{[\phi''(\bar{r}_0)]^4}\right)\right.\\&\left.+0.5\frac{[\phi'''(\bar{r}_0)]^3}{[\phi''(\bar{r}_0)]^4}[4\cos^2\tfrac{1}{4}kX^{-3/2}\Theta(X)+4\sin^2\tfrac{1}{4}kY^{-3/2}\Theta(Y)]\right]\,,\end{aligned} \tag{51}$$

$$\Gamma_4^{TE}=0.125\frac{\omega_k}{\beta}\omega aT\bar{r}_0\left[[X_1^{-1/2}\Theta(X_1)+Y_1^{-1/2}\Theta(Y_1)]\left(\frac{2\phi'''(\bar{r}_0)\phi''''(\bar{r}_0)}{[\phi''(\bar{r}_0)]^3}-2.5\frac{[\phi'''(\bar{r}_0)]^3}{[\phi''(\bar{r}_0)]^4}\right)\right]\,, \tag{52}$$

where a and b are defined through the thermal strain according to the relation

$$\eta=aT+bT^2\,. \tag{53}$$

The general expressions for a and b are now available[12] for a more realistic model than our model. The explicit anharmonic contributions to the phonon frequency shift and width are still given by the expressions of Sec. II A and II B, respectively, but it should be understood that the derivatives ϕ^n are now to be evaluated at $\bar{r}_0$.

IV. DISCUSSIONS AND CONCLUSIONS

In Sec. III we have obtained expressions for the anharmonic contributions to the phonon frequency shift and width. Some complicated contributions have been calculated only for $k=\pi$. At least for this model it has been clearly demonstrated that it is possible to have exact numerical results of $O(\lambda^4)$ for the phonon frequency shift and width. The contribution of $O(\lambda^4)$ to the inband phonon width is found to depend on the wave number, contrary to the corresponding width of $O(\lambda^2)$, which is known to be wave-number independent. In order to find the magnitude of each of the anharmonic contributions of $O(\lambda^4)$ to the phonon frequency shift and width we evaluate them for $\omega=\omega_k$ and $k=\pi$ using the Lennard-Jones potential. The calculated results for the phonon frequency shift and width are presented in Tables I(a) and I(b), respectively. In Table I(a) the first two rows give anharmonic contributions of $O(\lambda^2)$ whereas the third row is the thermal-expansion contribution of the same order to the phonon frequency shift. They are given in units of $\omega_L(k_BT/\epsilon_0)$. In Table I(b) the first row is the phonon width of $O(\lambda^2)$ in the same units. We have given lower-order results[13,14] for the sake of comparison and completeness. The last rows of Tables I(a) and I(b) are thermal-expansion contributions of $O(\lambda^4)$ to the phonon frequency shift and width, respectively. In the evaluation to $O(\lambda^4)$ of anharmonic contributions due to thermal expansion, we have used for our model $a=0.1458(k_B/\epsilon_0)$ and $b=0.2699(k_B/\epsilon_0)^2$, as obtained from free-energy expressions.[6,12] The remaining rows of the tables give the explicit anharmonic contribution of $O(\lambda^4)$ to the phonon frequency shift and width. These are given in units of $\omega_L(k_BT/\epsilon_0)^2$. It can be easily seen from the tables that the partial sums of the anharmonic contributions of $O(\lambda^4)$ to the phonon frequency shift and width in the various order of perturbation theory are of the same order of magnitude and there is strong cancellation among them. There are many anharmonic contributions of $O(\lambda^4)$. Therefore it seems difficult to predict *a priori* the importance of a particular anharmonic contribution in a given order of perturbation as all of them are of the same order of magnitude. Thus none of the anharmonic contributions of $O(\lambda^4)$ to the phonon frequency shift and width can be ignored. In view of this we feel that in order to find the temperature dependence of the fundamental lattice absorption peak in ionic crystals, the contributions of anharmonic terms of the same order should be taken into account instead of discussing the contributions of only a few diagrams.[1,2] Work on this is in progress and will be reported in a subsequent paper in this series.

TABLE I. Various anharmonic contributions to (a) the inband phonon frequency shift at $k=\pi$ and (b) the inband phonon width at $k=\pi$.

	Contributions	Values	Partial sums
(a)	Δ^{1a}	1.2882	
	Δ^{2a}	−1.5312	−1.7740
	Δ_2^{TE}	−1.5309	
	Δ^{1b}	1.3807	1.3807
	Δ^{2b}	−1.8229	
	Δ^{2c}	−3.3189	−13.8448
	Δ^{2d}	−6.5220	
	Δ^{2e}	−2.1740	
	Δ^{3a}	0.00	
	Δ^{3b}	3.9451	25.3551
	Δ^{3c}	17.4649	
	Δ^{3d}	3.9451	
	Δ^{4a}	−8.2783	−15.8694
	Δ^{4b}	−7.5910	
	Δ_4^{TE}	0.0043	0.0043
(b)	Γ^{2a}	1.5312	1.5312
	Γ^{2b}	7.1422	13.6643
	Γ^{2d}	6.5220	
	Γ^{3a}	−7.8902	−54.1005
	Γ^{3b}	−5.9176	
	Γ^{3c}	−40.2928	
	Γ^{4a}	24.3991	37.2951
	Γ^{4b}	10.8959	
	Γ_4^{TE}	3.8326	3.8326

Finally, we examine the convergence of our perturbation expansion for the present model. We find the ratios of the anharmonic shifts and widths of $O(\lambda^4)$ and $O(\lambda^2)$, respectively. These are found to be

$$\Delta(\lambda^4)/\Delta(\lambda^2)=1.6765(k_BT/\epsilon_0), \tag{54}$$

$$\Gamma(\lambda^4)/(\lambda^2)=0.4515(k_BT/\epsilon_0). \tag{55}$$

It is known that for inert-gas crystals the potential depth ϵ_0 is roughly twice the melting temperature. Therefore we conclude from Eqs. (54) and (55) that lower-order perturbation is inadequate for temperatures greater than about one third of the melting temperature. This is in agreement with previous conclusions.[4,9]

ACKNOWLEDGMENT

We are thankful to Dr. V. K. Jindal for providing values of the thermal-expansion coefficients a and b and for several useful discussions.

APPENDIX

In this Appendix the full expression for $H(x, k, \omega)$ occurring in the integral $I_R^{4b}(k, \omega)$ is presented.

For this, we define $\omega_2 = \sin(k' - x)$ and

$$a_1 = \sin k' - \sin x - \sin(k' - x), \quad \text{(A1)}$$

$$a_2 = \omega(\cos k' - \cos x) - p_2\omega_2(1 - \cos k'), \quad \text{(A2)}$$

$$a_3 = \omega(\sin k' - \sin x) + p_2\omega_2 \sin k', \quad \text{(A3)}$$

$$D_1 = a_3^2 + a_2^2 - a_1^2, \quad \text{(A4)}$$

$$T_1 = [a_1 \sin k' - \omega(a_2 \cos k' + a_3 \sin k')]/D_1, \quad \text{(A5)}$$

$$T_2 = \{a_1[\sin k' - \sin(k' - x)] - (\omega + p_2\omega_2) \times (a_2 \cos k' + a_3 \sin k')\}/D_1, \quad \text{(A6)}$$

$$a_4 = \sin k' - \sin x + \sin(k' - x), \quad \text{(A7)}$$

$$a_5 = \omega(\cos k' - \cos x) + p_2\omega_2(1 + \cos k'), \quad \text{(A8)}$$

$$D_2 = a_3^2 + a_5^2 - a_4^2, \quad \text{(A9)}$$

$$T_3 = [a_4 \sin k' - \omega(a_5 \cos k' + a_3 \sin k')]/D_2, \quad \text{(A10)}$$

$$T_4 = \{a_4[\sin k' + \sin(k' - x)] - (\omega + p_2\omega_2) \times (a_5 \cos k' + a_3 \sin k')\}/D_2, \quad \text{(A11)}$$

$$a_6 = \sin k' + \sin x + \sin(k' - x), \quad \text{(A12)}$$

$$a_7 = \omega(\cos k' + \cos x) - p_2\omega_2(1 - \cos k'), \quad \text{(A13)}$$

$$a_8 = \omega(\sin k' + \sin x) + p_2\omega_2 \sin k', \quad \text{(A14)}$$

$$D_3 = a_8^2 + a_7^2 - a_6^2, \quad \text{(A15)}$$

$$T_5 = [a_6 \sin k' - \omega(a_7 \cos k' + a_8 \sin k')]/D_3, \quad \text{(A16)}$$

$$T_6 = \{a_6[\sin k' + \sin(k' - x)] - (\omega + p_2\omega_2) \times (a_7 \cos k' + a_8 \sin k')\}/D_3, \quad \text{(A17)}$$

$$a_9 = \sin k' + \sin x - \sin(k' - x), \quad \text{(A18)}$$

$$a_{10} = \omega(\cos k' + \cos x) + p_2\omega_2(1 + \cos k'), \quad \text{(A19)}$$

$$D_4 = a_8^2 + a_{10}^2 - a_9^2, \quad \text{(A20)}$$

$$T_7 = [a_9 \sin k' - \omega(a_{10} \cos k' + a_8 \sin k')]/D_4, \quad \text{(A21)}$$

$$T_8 = \{a_9[\sin k' - \sin(k' - x)] - (\omega + p_2\omega_2) \times (a_{10} \cos k' + a_8 \sin k')\}/D_4, \quad \text{(A22)}$$

$$X_2 = (\omega + p_2\omega_2)^2 - 2(1 + \cos x), \quad \text{(A23)}$$

$$Y_2 = (\omega + p_2\omega_2)^2 - 2(1 - \cos x), \quad \text{(A24)}$$

Using above notations, $H(x, k, \omega)$ can be written as

$$H(x, k, \omega) = (T_1 + T_5)Y^{-1/2}\Theta(Y) + (T_3 + T_7)X^{-1/2}\Theta(X) - (T_2 + T_8)Y_2^{-1/2}\Theta(Y_2) - (T_4 + T_6)X_2^{-1/2}\Theta(X_2), \quad \text{(A25)}$$

The integrand $H_1(x, k, \omega)$ occurring in the integral $I_G^{4b}(k, \omega)$ can be obtained from Eq. (A25) by replacing X by X_1, Y by Y_1, X_2 by $-X_2$, and Y_2 by $-Y_2$.

---

*Supported in part by U. S. NSF under Grant No. GF-36470.

[1]I. P. Ipatova, A. A. Maradudin, and R. F. Wallis, Fiz. Tverd. Tela. 8, 1064 (1966) [Sov. Phys. Solid State 8, 850 (1966)]; Phys. Rev. 155, 882 (1967).

[2]A. D. Bruce, J. Phys. C 6, 174 (1973).

[3]K. N. Pathak and Y. P. Yarshni, Phys. Lett. A 23, 539 (1969); K. G. Aggarwal and K. N. Pathak, *ibid.* 35, 255 (1971).

[4]R. C. Shukla and E. R. Cowley, Phys. Rev. B 3, 4055 (1971); R. C. Shukla and L. Wilk, *ibid.* 10, 3660 (1974).

[5]K. G. Aggarwal and K. N. Pathak, Phys. Rev. B 7, 4449 (1973); K. G. Aggarwal, *ibid.* 8, 5867 (1973).

[6]M. R. Monga and V. K. Jindal, Phys. Rev. B 11, 1718 (1975).

[7]R. S. Tripathi and K. N. Pathak, Nuovo Cimento 21, 289 (1974).

[8]M. R. Monga and K. N. Pathak (unpublished).

[9]M. R. Monga, K. C. Sharma, and K. N. Pathak (unpublished).

[10]M. R. Monga, V. K. Jindal, and K. N. Pathak, Nucl. Phys. Solid State Phys. Symp. (India) 17C, 184 (1974).

[11]The numerical factor appearing in Eq. (26a) of I should be multiplied by 2.

[12]V. K. Jindal and K. N. Pathak, Phys. Rev. B 11, 972 (1975), and *ibid.* (to be published).

[13]K. N. Pathak, Phys. Rev. A 139, 1569 (1965).

[14]A. A. Maradudin, Phys. Lett. 2, 298 (1962).

[15]N. M. Plakida and T. Siklos, Phys. Status Solidi 33, 113 (1969).